

Rietveld analysis of XR data, other structural and temperature dependent dielectric properties of BaTiO₃

Dharmendra Mewada, and Rajesh Kumar Katare

Department of Physics, SAGE University, Indore (M.P.), 452020, India

Abstract:

For energy storage devices, BaTiO₃ is a suitable material as it inherits higher resistance to temperature, low loss character and ability to store larger amount of energy. In this work, we discuss the synthesis, Rietveld analysis of diffraction data, other structural properties in addition to the polarization and temperature dependent dielectric properties. Sample was synthesized by solid state route and XRD data studies confirm the tetragonal structure acquired. The results of XRD were verified by the Raman and FTIR analysis. The Curie temperature i.e. the transition temperature where tetragonal phase acquires cubic phase was found to be $T_c = 365\text{K}$. Furthermore, polarization studies revealed the sample to exhibit weak polarization with leakage current features.

Keywords: Rietveld refinement, high temperature dielectric properties, Transition temperature, polarization

Introduction

The larger energy storage ability, low loss and good temperature stability has a great technological importance in the development of energy storage devices in engineering science. With the recent growing demand of environmental protection, materials with lead-free compositions attracted much interest to substitute for the lead-based ferroelectrics. The dielectric ceramic materials have potential in electronic ceramic industry attributed to above mentioned salient desired features [1-4]. BaTiO₃, the first ferroelectric perovskite material discovered inherits higher dielectric constant. It inherits three structural phase transitions. To be influential in the applications of sensors, actuators, transducers and transformers due to the lack of coping of a giant piezoelectric response, the various technological challenges that come in between needs to be addressed first. Among these challenges, the T_c , piezoelectric response, electromechanical coupling, electrical resistivity, mechanical and electrical quality factor, dielectric permittivity and thermal stability are various issues that must be optimized simultaneously [5-7].

Barium titanate (BaTiO₃) exhibits a phase transition from cubic phase (paraelectric) to tetragonal phase (ferroelectric) at 120°C. BaTiO₃ ceramic has high dielectric permittivity and inherits a sharp dielectric anomaly at the phase transition point which put barriers in its application in advanced technologies. Due to low T_c value and diffuse phase transition, BaTiO₃-based ceramics have attracted the keen attention of the researchers attention. In the fabrication of storage devices, these materials with high dielectric constant and low dielectric loss is useful [8-10].

The intriguing features arise from the synthesis route, purity, density, grain size, temperature, frequency and dopants etc. For fundamental technological interest, BaTiO₃ powders with narrow particle size distribution, controlled morphology, and high purity were studied intensively. The factors that hurdle the advanced applications are chemical inhomogeneity and varied reactivity BTO samples using various preparation techniques. These issues arise as these methods result in a grain size of wide range, without any control on shape, morphology and size of particles [11-13]. It is however worth to mention here that there is no method that works perfectly. Therefore we selected solid state route to synthesize the sample. This method yields single phase material with lesser chance of impurity. Furthermore this technique provides better control over phase formation, crystallinity, and dispersibility of particles in the sample.

Synthesis

The BaTiO₃ ceramic materials were synthesized by solid state method through double calcination process. The starting materials were powdered by grinding using agate mortar-pestle and the mixture ground for 5h in each calcination of 1000 °C and 1200 °C for 10h. To get fine powder in final, the calcined mixture was ground for 1h. The powder was transformed to pellet form with thickness of 1mm and diameter in 10mm. To emphasize on electrical properties, the pellets were treated at higher temperature to form compact material (sintered at 1300 °C for 10 h).

Experimentation

The crystal structure acquired by the sample was confirmed from X-ray powder diffraction technique using Bruker D8-Advance X-ray diffractometer with CuK α 1 ($\lambda=1.5406 \text{ \AA}$) radiation. To ascertain the phase, we performed Raman inelastic spectral measurement using Micro Raman System from JobinYvon Horiba LABRAM-HR visible (400–1100 nm) with excitation source as argon (488 nm). Perkin Elmer FT-IR/FIR spectrometer was employed to record Fourier transform infrared spectra (FTIR) in the range of 400

cm⁻¹ to 4000 cm⁻¹. The Precision LCR meter (2Hz-2MHz), Model E4980A from Keysight Technologies was used for dielectric measurements. Loop tracer make of M/s Radiant Instruments, USA was exploited to record the electrical polarization vs field (P-E loop) data

Results and Discussions

XRD analysis

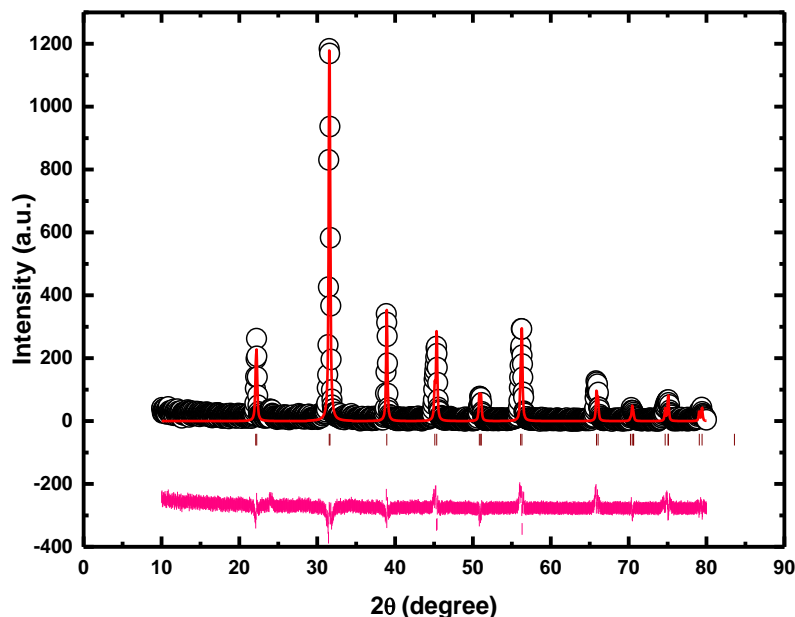


Figure 1: Rietveld refinement of XRD data of BaTiO₃

The BaTiO₃ was investigated for structure and type of phase acquired by the materials via the X-ray diffraction data analysis. The data was refined using FullProf software to throw light on the crystal structure acquired and tabulate other structural parameters. Rietveld refinement reveals that the sample is single phased and has acquired tetragonal phase of space group P4mm[14,15]. However, the intense reflection peaks as Figure1 displays, are attributed to the higher crystallinity in the sample. Whereas higher average crystallite size in the sample can be predicted from narrow FWHM of the reflection peaks. The various structural parameters obtained from the refinement of the XRD data of BaTiO₃ are given in Table 1.

Raman Studies

For non-centrosymmetric structures, Raman spectroscopic technique is an effective tool. It provides information about tetragonal phase for the sample under observation. The Raman spectra were recorded in the range 100 cm⁻¹ to 1000 cm⁻¹.

Figure 2 displays Raman spectrum of the BaTiO₃ ceramic material[16,17]. The characteristic bands related to tetragonal BTO based compounds are evident from the Raman spectrum.

| Table 1: Structural Parameters obtained from Rietveld refinement | | |
|--|-------------|-------------------------|
| S. No. | Parameters | values |
| 1 | Structure | Tetragonal |
| 2 | Space group | P 4 m m |
| 3 | $a=b$ | 3.9966 Å |
| 4 | c | 4.0168 Å |
| 5 | volume | 64.1604 Å ³ |
| 6 | density | 6.036 g/cm ³ |
| 7 | GOF | 2.2 |
| 8 | χ^2 | 1.56 |

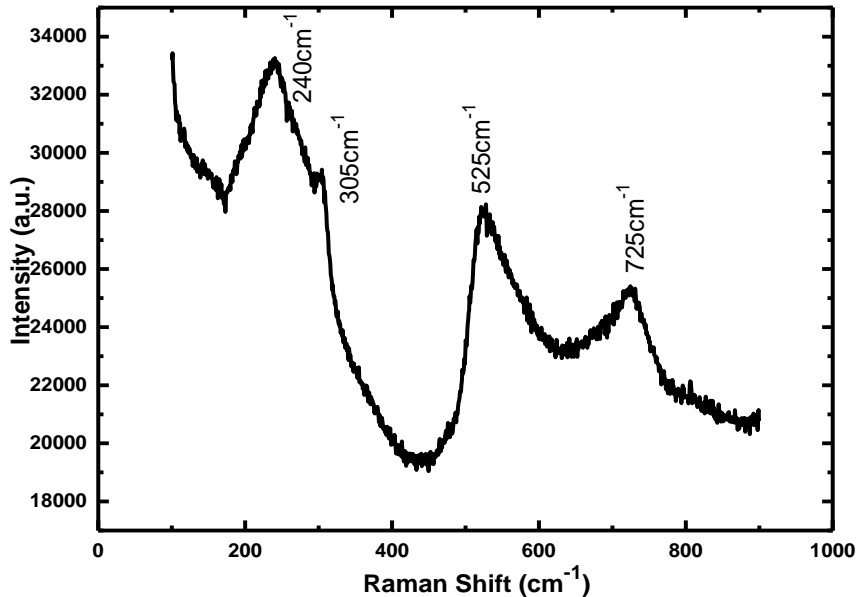


Figure 2: Raman spectrum of BaTiO₃

The acquisition of tetragonal phase is indicated by the presence of vibration mode at 305 cm⁻¹. The fundamental transverse optical (TO) phonon mode of A₁ symmetry are witnessed via appearance of peaks at 240 cm⁻¹ and at 525 cm⁻¹ which is an asymmetric peak. The phonon mode appearing at 305 cm⁻¹ that indicates the asymmetry of TiO₆ octahedra with BaTiO₃ structure is an attribute of [B₁, E(TO+LO)] mode. The phonon mode existing at 720 cm⁻¹ has A₁ symmetry and represented as [A₁(LO), E(LO)] mode. This phonon mode is related to highest frequency longitudinal optical (LO) mode [16-19]. The Raman spectrum this confirms the tetragonal phase of the sample and thereby agrees with revelations of XRD analysis of the sample.

FTIR Studies

Figure 3 displays the FTIR spectrum of BaTiO₃. The spectrum is measured as % Transmittance vs wavenumber in the range of 400 cm⁻¹ – 4000 cm⁻¹. The FTIR absorption bands visible about 860 cm⁻¹ and 1440 cm⁻¹ arise due to vibration bands of CO₃²⁻ groups. Corresponding to Ti-O bond, the absorption band appears at 400 cm⁻¹ whereas mode of vibration about 500 cm⁻¹ is attributed to Ba-O bonds. Due to moisture in the sample, the absorption bands appearing at 1090 cm⁻¹ and at 2975 cm⁻¹ are attributed to O-H, the hydroxyl group. The FTIR spectral analysis hence confirms the desired sample formation and the results are in agreement with the available literature [20-22].

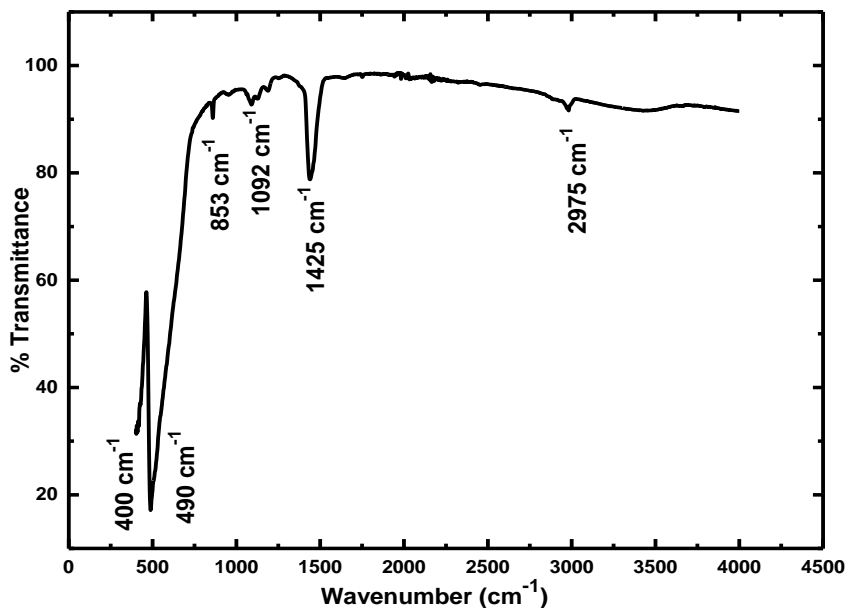


Figure 3: Fourier Transform Infra-red spectrum of BaTiO₃

Dielectric Studies

Figure 4 shows the temperature dependence of the dielectric constant (ϵ) of BaTiO₃ at 0.5 and 1 kHz. The dielectric constant increases with an increase of temperature up to Curie temperature (T_c) and then decreases. Since the charge hopping is a thermally activated process, dielectric polarization increases with increasing temperature, resulting in an increase of the dielectric constant. The dielectric constant (ϵ) of a material has 4 polarization contributions: electronic polarization (ϵ_e), ionic polarization (ϵ_i), dipolar polarization (ϵ_d), and space-charge polarization (ϵ_s). Response frequencies for electronic and ionic polarization are $\sim 10^{16}$ and 10^{13} Hz, respectively, and at frequencies above 100 kHz, contribution from space-charge polarization is not expected [23,24]. This saturation of space-charge polarization results in low dielectric constant values at higher frequencies.

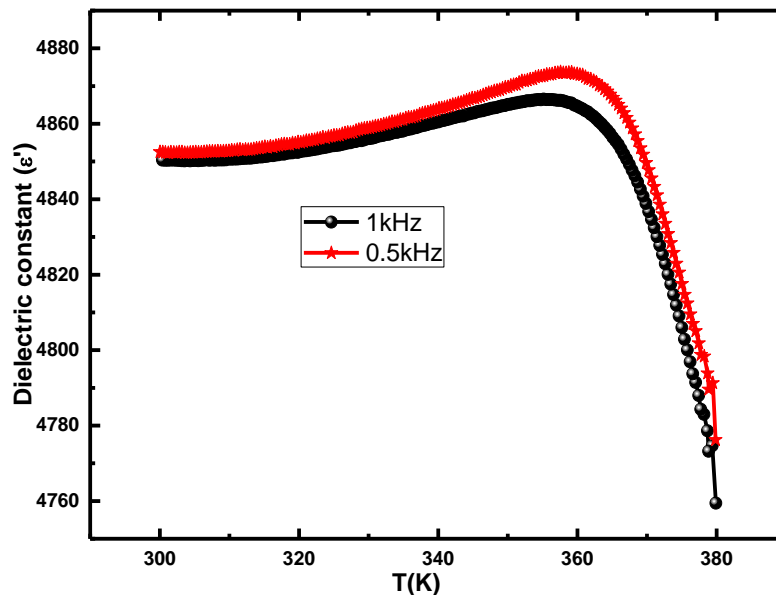


Figure 4: High temperature dielectric responsive character of BaTiO₃ at constant values of frequencies

As frequency is increased, the dielectric constant is observed to decrease which is a normal behaviour of these materials. At lower frequencies, the dipolar and interfacial polarizations contribute significantly to the dielectric constant. Both of these are temperature-sensitive; hence, the dielectric constant increases at high rates for lower frequencies compared to higher frequencies. At high frequencies only electronic polarization becomes significant, rather than dipolar [25,26].

The signature of ferroelectric to the paraelectric phase transition is clearly visible and exactly similar behaviour has been reported earlier [26,27]. It can be observed from Figure 4 that the Curie temperature (T_c) for BaTiO₃ was nearly 366K at 1 kHz. The rise in T_c is attributed to the larger grain size. It was reported that a close relation exists between the Curie temperature and internal stresses developed in the constrained grains at the phase transition temperature. The internal stress can shift the T_c to higher temperatures with increased grain size [28-30]. Corresponding to transition temperature, we say below it the materials is tetragonal and above it the sample acquires cubic structure

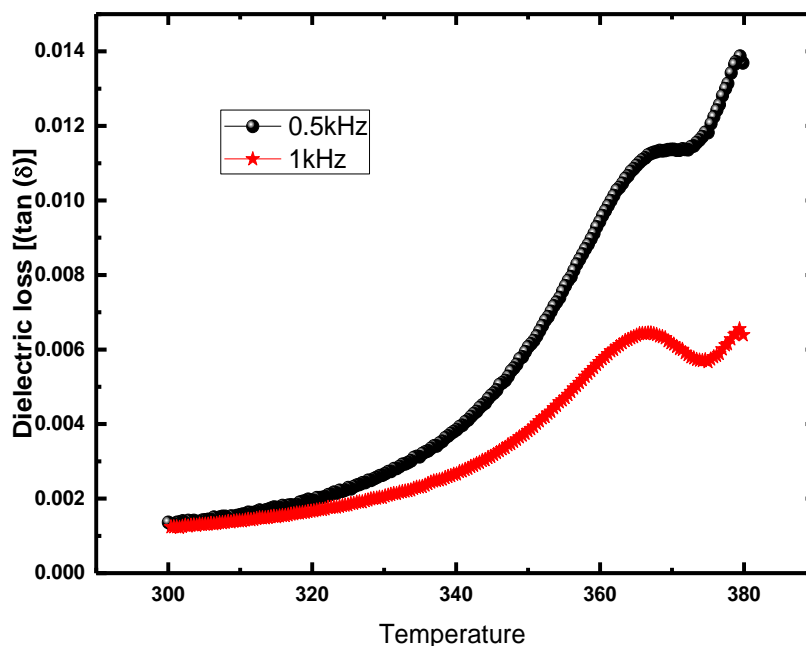


Figure 5: Temperature dependent dielectric loss of BaTiO₃

It is clear from Figure 5 that the value of the dielectric loss increases with increasing temperature. A phase transition in cubic phase is observed about 370K and after the phase change from tetragonal phase to cubic phase, the, $\tan(\delta)$ decreases with increase in temperature. Corresponding to 375K, we again observed increase in dielectric loss with increase in temperature. This further indicates a new transition from cubic to tetragonal phase. Furthermore, it is most note behaviour that increase in the applied field value has reduced dielectric constant similar case to that of dielectric constant[31-32].

Polarization (P-E loop)Studies

Since BaTiO₃ is a well-known ferroelectric material, we investigated its ferroelectric properties. The induced polarization (P-E loop) as a function of electric field ranging from -25kV/cm to +25kV/cm at a constant potential of 1500V displayed as Figure 6. The leakage current is evident from the incomplete P-E loop, the lack of sharp saturation as well as weak polarization is exhibited by sample in addition. Higher coercive field about 4.3 kV/cm, remnant polarization (0.07 μ C/cm²) with saturation of the order of 0.32 μ C/cm². The week polarization of the sample as observed may be attributed to the large structural inhomogeneities and lattice distortions induced by severe grinding and higher temperature treatment. Morphology where porosity may be the other responsible factor for the observed week polarization[33-35]

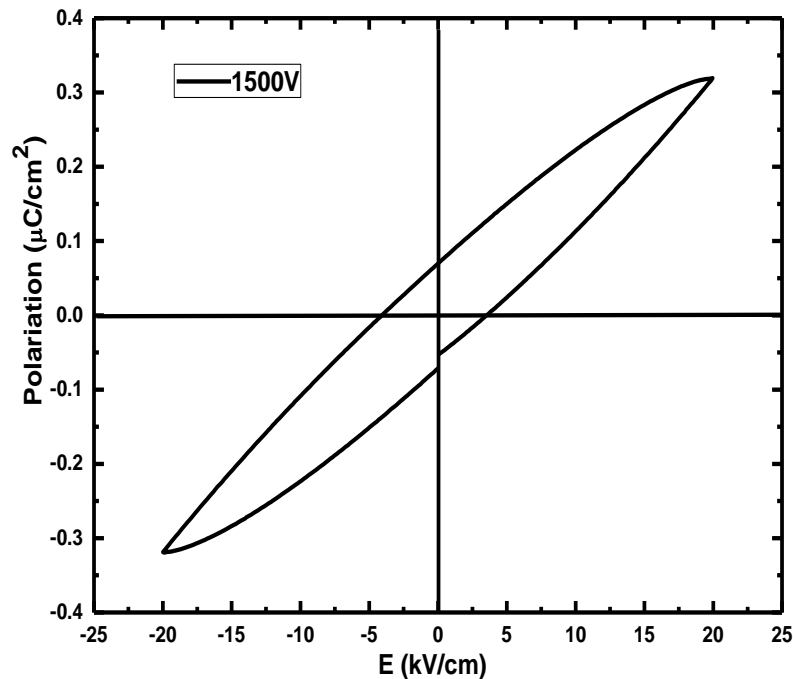


Figure 6: Polarization (P-E) loop of BaTiO₃

In conclusion, the successfully synthesized samples was found to inherit tetragonal phase. The sample formation was conveyed from analysis of Raman and FTIR data also. Temperature dielectric analysis inferred the sample have high dielectric constant with very low dissipation. The transition was witnessed about $T_c = 365$ K. Above this critical temperature, the dielectric constant as well as dielectric loss falls. The P-E loop studies revealed the sample to exhibit low polarization attributed to structural inhomogeneities and distortions induced during sintering and grinding.

Acknowledgement

Authors acknowledge institute UGC-DAE-CSR Indore for extending characterization facilities. Dr. N. Kaurav, Govt Holkar Science College, Indore for guidance and facility for sample preparation.

References

- [1] B. Luo, X. Wang, E. Tian, G. Li, L. Li, J. Mater. Chem. C 3 (2015) 8625.
- [2] S.H. Wemple, M. Didomenico, I. Camlibel, J. Phys. Chem. Solid. 29 (1968) 1797.
- [3] G.H. Haertling, J. Am. Ceram. Soc. 82 (1999) 797.
- [4] K. Yang, X. Huang, Y. Huang, L. Xie, P. Jiang, Chem. Mater. 25 (2013) 2327.
- [5] G. H. Haertling, Journal of the American Ceramic Society, 82(1999)797-818
- [6]C.A. Miller, Br. J. Appl. Phys. 18 (1967) 1689.

- [7] M. T. Buscaglia, M. Viviani, V. Buscaglia, C. Bottino and P. Nanni, *Journal of the American Ceramic Society*, 85 (2002) 1569-1575
- [8] P. Yongping, Y. Wenhui, and C. Shoutian, *Journal of Rare Earths*, 25, (2007)154-157
- [9] Y. Leyet, R. Peña, Y. Zulueta, F. Guerrero, J. Anglada-Rivera, Y. Romaguera, and J. P. Cruz, *Materials Science and Engineering: B*, 177(2012) 832-837
- [10] N. A. Hamid, R. A. M. Osman, M. S. Idris and T.Q. Tan, *Materials Science Forum*, 819 (2015).
- [11] S. Roberts, *Phys. Rev.* 71 (1947) 890.
- [12] A. von Hippel, *Rev. Mod. Phys.* 22 (1950) 221.
- [13] H. Xu, L. Gao, *J. Am. Ceram. Soc.* 86 (2003) 203.
- [14] M. Soni et al., *Journal of Molecular and Engineering Materials*, 8, (2020) 2050004
- [15] C. Chen, H. Zhuang, X. Zhu, D. Zhang, K. Zhou, H. Yan, *J Mater Sci: Mater Electron* 26 (2015) 2486–2492
- [16] H. A. Avila, L. A. Ramajo, M. M. Reboredo, M. S. Castro and R. Patra, *Ceram. Int.* 37 (2011) 2383
- [17] L. Huang, Z. Chen, J. D. Wilson, S. Benerjee, R. D. Robinson, I. P. Hermen, R. Labowitz and S. O'Brien, *J. Appl. Phys.* 100 (2006) 034316
- [18] T. Badapanda S. Venkatesan, S. Panigrahi, S. Anwar, 31(2013) 1-6.
- [19] M. Singh, C. Yadav, A. Ranjan M. Kaur, SK Gupta, *Sensors and Actuators B*, 241 (2017)1170
- [20] A. Maqbool, A. Hussain, R.A. Malik, J.U. Rahman, A. Zaman, T.K. Song, M.H. Kim, *Mater. Sci. Eng. B* 199, (2015)105–112
- [21] M. Saleem, S. Tiwari, M. Soni, N. Bajpai and A. Mishra, *Int. J. Mod. Phys. B.* 33 (2020)2050033
- [22] PTT Mai, et al. *Journal of Science and Advanced Devices* , 1 (2016) 90-97
- [23] K. Yao, L. Zhang, X. Yao, W. Zhu, *J. Mater. Sci.* 32 (1997) 3659–3665
- [24] D. McCauley, R.E. Newnham, C.A. Randall, *J. Am. Ceram. Soc.* 81 (1998)979–987
- [25] Lines, M. E.; Glass, A. M. *Principles and Applications of Ferroelectric and Related Materials* ; Oxford: Clarendon Press, 2001.
- [26] Rukmini, H. R.; Choudhary, R. N. P.; Prabhakara, D. L. *Mater. Chem. Phys.* 64 (2000) 171–178.
- [27] Hwang, H. J.; Nagai, T.; Ohji, T.; Sando, M. *J. Am. Ceram. Soc.* 81 (1998)709–712.
- [28] V. Mishra, A. Sagdeo, V. Kumar, M.K. Warshi, H.M. Rai, S.K. Saxena, D.R. Roy, V. Mishra, R. Kumar, P.R. Sagdeo, *J. Appl. Phys.* 122 (2017), 065105.
- [29] A. Sagdeo, A. Nagwanshi, P. Pokhriyal, A.K. Sinha, P. Rajput, V. Mishra, P. R. Sagdeo, *J. Appl. Phys.* 123 (2018) 161424.
- [30] N.-H. Chan, R.K. Sharma, D.M. Smyth, *J. Am. Ceram. Soc.* 65 (1982) 167.
- [31] X. Aupi, J. Breeze, N. Ljepojevic, L.J. Dunne, N. Malde, A.-K. Axelsson, N. McN. Alford, *J. Appl. Phys.* 95 (2004) 2639.
- [32] M. Sparks, D.F. King, D.L. Mills, *Phys. Rev. B* 26 (1982) 6987.
- [33] Y. Tan, J. Zhang, Y. Wu et. al., *Scientific Reports*, 5 (2015) 9953
- [34] A. Hussain, A. Maqbool, R.A. Malik, J.-H. Lee, Y.S. Sung, T.K. Song, M.H. Kim, *Ceram. Int.* 43 (2017) S204–S208
- [35] R.A. Malik, A. Hussain, A. Maqbool, A. Zaman, C.W. Ahn, J.U. Rahman, T.K. Song, W.J. Kim, M.H. Kim, *J. Am. Ceram. Soc.* 98 (2015)3842–3848